The Indonesian Journal of Computer Science
www.ijcs.net
Volume 13, Issue 6, December 2024
https://doi.org/10.33022/ijcs.v13i6.4489

Design and Development of a Hybrid Tricopter Fixed-Wing UAV for Precision Agriculture

Rokhmat Febrianto[1*], Jessie Charydon Yeoh[2], I Gede Arinata Kusuma Putra[3], Ayomi Sasmito[4], Agung Alfiansyah[5]
[1*]rokhmat.febrianto@prasetiyamulya.ac.id, [2]23402310002@student.prasetiyamulya.ac.id, [3]23402310001@student.prasetiyamulya.ac.id, [4]ayomi.sasmito@prasetiyamulya.ac.id, [5]agung.alfiansyah@prasetiyamulya.ac.id
[1,2,3,5]Department of Computer Systems Engineering, Universitas Prasetiya Mulya, Indonesia
[4]Department of Mathematics, Universitas Prasetiya Mulya, Indonesia

Article Information

Received : 6 Nov 2024
Revised : 4 Dec 2024
Accepted : 30 Dec 2024

Keywords

UAV, Tricopter, PID Control, Precision Agriculture, Tilt Rotor

Abstract

Precision Agriculture (PA) relies on innovative technologies to enhance efficiency and sustainability in agricultural practices. This study focuses on the design, simulation, and evaluation of a Hybrid Tricopter VTOL UAV tailored for PA applications. The UAV combines hover and fixed-wing flight modes, enabling versatility in data collection and farmland monitoring. Through rigorous simulations, the hover mission demonstrated the effectiveness of PID controllers in stabilizing roll, pitch, and yaw dynamics, achieving high positional accuracy with minimal error rates. The transition mission validated the UAV's adaptability, showcasing smooth transitions between flight modes under varying tilt rates. Additionally, electronic component simulations confirmed the propulsion system operates efficiently within thermal and electrical limits, ensuring durability and energy efficiency. The findings highlight the UAV's reliability, adaptability, and operational readiness, laying a foundation for advanced UAV applications in PA and beyond. This work underscores the potential of UAVs in optimizing agricultural productivity and sustainability.

A. Introduction

Precision Agriculture (PA) represents a structured and data-driven methodology aimed at enhancing the effectiveness of agricultural practices. As described by the International Society of Precision Agriculture (ISPA) in January 2024, PA involves the systematic gathering, processing, and evaluation of temporal, spatial, and specific data on plants and animals. This information is integrated with other relevant insights to support informed decision-making [1]. The primary aim of PA is to optimize the use of resources, boost productivity, improve quality, and increase profitability while promoting the sustainability of agricultural production systems. By addressing the inherent variability within farming environments, PA strives to maximize agricultural yields with minimal resource usage or, alternatively, maximize output relative to input. This approach serves as a modern strategy to tackle the challenges of efficient and sustainable agriculture.

A recent report from the United Nations highlighted growing concerns regarding global agricultural production trends, population growth, and shifting consumption patterns [2]. Efforts to increase food production are often constrained by inefficient practices that harm the environment, exacerbating the dependency on climatic conditions, which can negatively impact crop yields. These issues call for a paradigm shift in agricultural practices and a reevaluation of agriculture's role in society.

Efficiency in agriculture is critical for ensuring the steady production of staple foods. Although advancements in Artificial Intelligence (AI) provide hope for addressing food insecurity [3], challenges related to global food availability remain unresolved. For instance, rice paddies, which are crucial for rice cultivation, are notoriously difficult to manage due to varying requirements throughout the crop's growth stages. Even minor variations in water levels can have detrimental effects on final yields, necessitating intensive care and intelligent engineering solutions to manage these fields [4].

	Jan	Feb	Mar	Apr	Mei	Jun	Jul	Ags	Sep	Okt	Nov	Des
2022	0,47	0,77	1,76	1,42	0,83	0,87	0,93	0,81	0,84	0,79	0,61	0,36
2023	0,45	0,94	1,65	1,17	0,97	0,95	0,83	0,86	0,84	0,70	0,50	0,35
2024	0,29	0,48	1,16	1,59								

Figure 1. Development of Rice Harvested Area in Indonesia (million hectares), 2022-2024 [5].

The importance of agricultural efficiency is further emphasized by data on rice production in Indonesia. As shown in Figure 1, the harvested area of rice in 2023 was approximately 10.21 million hectares, representing a decrease of 238.97 thousand hectares (2.29%) from the 2022 figure of 10.45 million hectares. The Indonesian Central Bureau of Statistics (BPS) attributes this decline to unfavorable climatic conditions and pest infestations, which have reduced the area available for rice cultivation in 2023. Additionally, labor shortages pose a significant challenge, exacerbated by the decreasing interest of younger generations in pursuing careers or involvement in agricultural activities [5].

Given the background and the challenges outlined, there is a clear gap in the utilization of technology that could be harnessed to improve the welfare of communities involved in agriculture. Remote sensing technologies play a critical role, especially given the vast scale of agricultural operations. In the context of Precision Agriculture, remote sensing can be achieved using satellites or Unmanned Aerial Vehicles (UAVs), which provide comprehensive aerial views of farmland. UAVs equipped with specialized cameras and algorithms enable the efficient collection of essential data, generating actionable insights for farm management. For example, UAVs can assist in tasks such as vegetation index analysis, hydrological mapping, crop stress evaluation, disease mapping, weed growth monitoring, and basic land surveying [6]. Furthermore, UAVs are often more practical and cost-effective than satellite-based remote sensing [7].

To enhance the effectiveness of Precision Agriculture, the development of UAVs capable of performing extensive farmland monitoring is crucial. By deploying these UAVs, farmers and agricultural managers can obtain accurate, real-time information about the condition of their land, allowing them to make informed decisions that enhance productivity and sustainability.

B. Related Works

There are two main types of UAV platforms: fixed-wing and rotary-wing. Fixed-wing UAVs resemble airplanes and operate by generating thrust and aerodynamic lift. These UAVs are generally larger in size compared to rotary-wing types and are often utilized for extensive applications like aerial spraying and photography [8], [9], [10], [11]. Rotary-wing UAVs, in contrast, can be categorized into helicopter and multi-rotor types. Helicopter-style UAVs are equipped with a single large rotor positioned on top, making them ideal for activities like aerial photography and spraying [12], [13], [14], [15]. Multi-rotor models are named according to the number of rotors they possess, with a "quadcopter" having four rotors [16], [17], [18], a hexacopter having six rotors [19], [20], and an octocopter having eight rotors [21]. Figure 2 illustrates several examples of UAVs that have been developed for remote sensing purposes.

Figure 2. Examples of UAVs used for remote sensing [6].
(a) Fixed-wing, (b) Rotary-wing.

The advantages of fixed-wing UAVs include their longer range, high energy efficiency, and faster speeds, as they utilize aerodynamic principles to generate lift without expending excessive energy. Conversely, rotary-wing UAVs excel in their maneuverability, especially in confined spaces, and are relatively easy to operate. In previous research, the fixed-wing Skywalker model, equipped with four propellers on both wings, was developed, as shown in Figure 3. This aircraft features four rotors and propellers to generate lift, along with an additional rotor and propeller to provide thrust [22]. However, the use of four propellers was deemed excessive and negatively impacted energy efficiency.

Figure 3. Skywalker Fixed-Wing UAV [23].

To address the challenges posed by the "Problem-Solving Approach" and leverage the strengths of both fixed-wing and rotary-wing UAVs, this research focuses on the development of a Hybrid Tricopter Fixed-Wing UAV. This hybrid design combines the characteristics of fixed-wing and rotary-wing configurations, making it particularly well-suited for monitoring missions as well as aerial image and video capture in agricultural environments. The Hybrid Tricopter's advantage lies in its ability to fly efficiently in fixed-wing mode, while also seamlessly transitioning to rotary-wing mode for enhanced maneuverability. Moreover, this UAV can take off and land vertically without requiring a runway, and it boasts a wide operational range, making it ideal for use in extreme terrains.

In its design, the UAV will be equipped with essential components such as sensors, actuators, and control systems to support its performance. The construction of the UAV will employ strong plastic materials, such as lightweight Polylactic Acid (PLA), and advanced 3D printing technology to ensure the structure aligns with the overall design. With these features, the Hybrid Tricopter stands out as a unique UAV platform, offering low power consumption, cost-effective production, minimal human safety risks, and substantial potential for applications in the agricultural sector.

C. Design concept of the system

The design concept of the Hybrid Tricopter VTOL UAV system combines the strengths of fixed-wing and rotary-wing architectures, optimizing versatility and efficiency for precision agriculture applications. This UAV is designed to operate in three primary modes: Tricopter Mode, Fixed-Wing Mode, and Transition Modes for take-off and landing. Tricopter Mode is utilized during vertical take-off and landing operations, allowing the UAV to hover and ascend or descend vertically, making it suitable for environments with limited space or where runways are unavailable. Fixed-Wing Mode, on the other hand, employs aerodynamic lift for forward flight, reducing energy consumption and extending flight endurance, making it ideal for

large-scale data collection missions. Transition Modes enable seamless shifts between vertical and horizontal orientations, ensuring smooth take-off and landing processes. The operational logic is governed by the pitch angle, which determines the active flight mode and ensures stable altitude adjustments during transitions. A clearer depiction of this operational logic and mode transitions can be seen in Figure 1, which provides a visual representation of the system workflow.

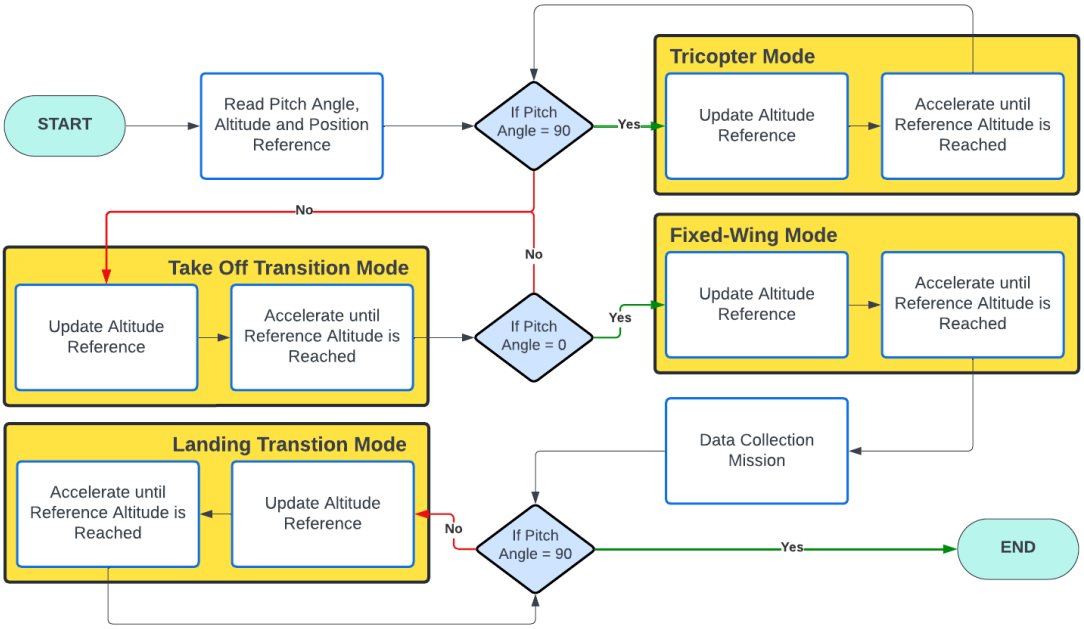

Figure 4. UAV Control System Workflow

The UAV's mechanical design prioritizes weight optimization, structural strength, and aerodynamic performance. The frame is constructed from lightweight Polylactic Acid (PLA) material, leveraging advanced 3D printing technology to create a robust yet lightweight structure. The propulsion system includes three high-efficiency brushless DC motors (BLDC) for the tricopter configuration, complemented by additional components for fixed-wing thrust. Strategic placement of propellers ensures optimal thrust-to-weight ratios and balance. Control surfaces, such as ailerons, elevators, and rudders, enable precise maneuvering during forward flight, while retractable landing gear reduces drag and provides stable support during VTOL operations. These features ensure that the UAV meets the demands of hybrid operations, offering durability, efficiency, and reliability.

The control and sensor systems are designed to ensure seamless hybrid operations. A Pixhawk Cube Orange flight controller processes inputs from onboard sensors to manage motor operations and execute mode transitions. Sensors, including pitch angle sensors, GPS modules, and accelerometers, provide real-time feedback for navigation and stability. Electronic Speed Controllers (ESCs) regulate motor speeds to facilitate smooth transitions and stable flight across all modes. The UAV is powered by a high-capacity Lithium Polymer (LiPo) battery, optimized for extended operations with safety features such as voltage cut-off to prevent over-

discharge. These systems work together to maintain operational stability, precision, and energy efficiency throughout the UAV's missions.

The operational workflow begins with an initialization phase, where the system reads pitch angle, altitude, and positional references to determine the appropriate flight mode. During the Take-Off Transition Mode, the UAV ascends vertically while gradually adjusting its pitch angle to transition into Fixed-Wing Mode. In Fixed-Wing Mode, the UAV maintains a horizontal orientation, using aerodynamic lift to sustain stable altitude and execute its data collection mission. Upon mission completion, the UAV transitions back to Landing Transition Mode, decelerating and adjusting its pitch angle to return to a vertical orientation for safe landing. The workflow ensures precise and efficient operations in various environments, from confined spaces to open agricultural fields.

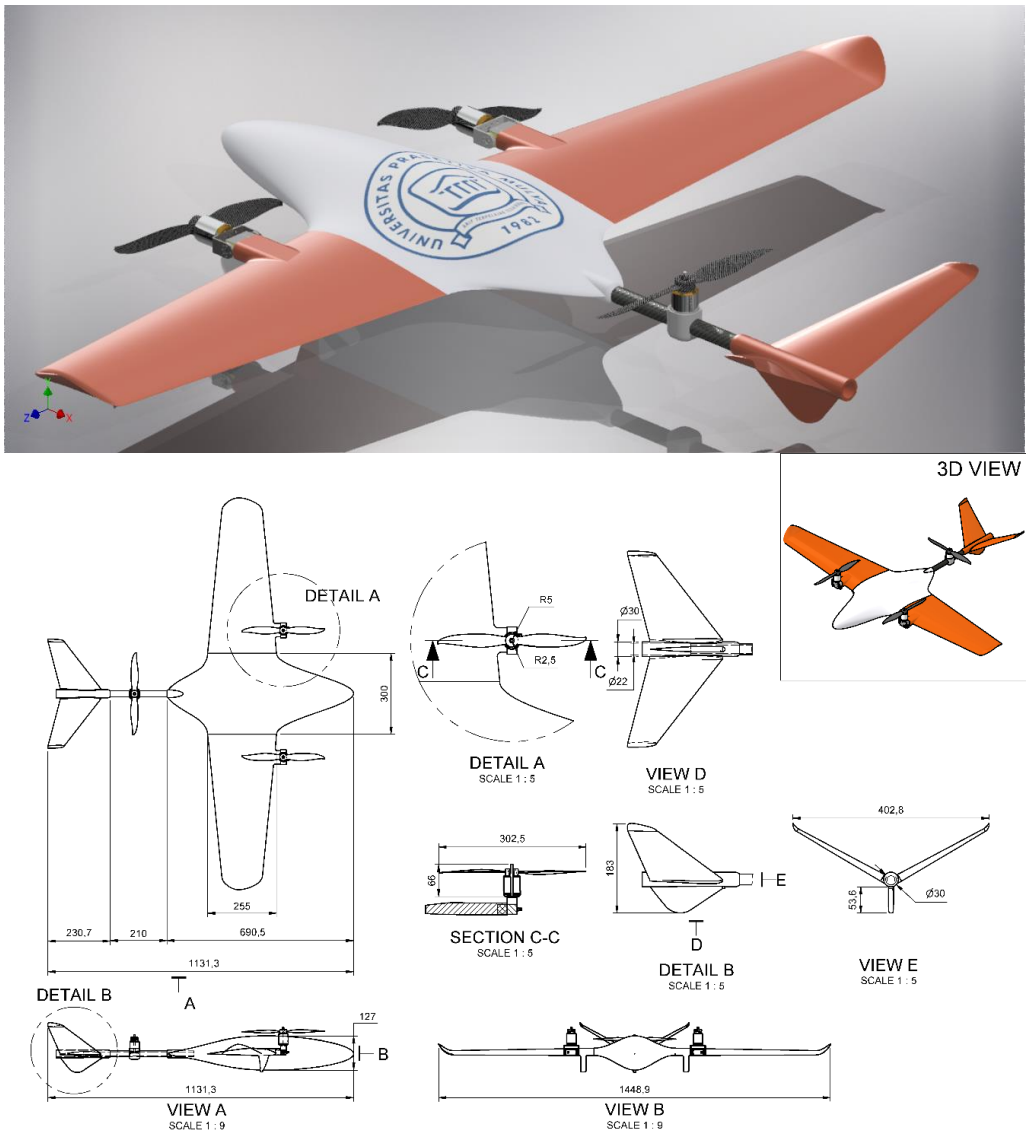

Figure 5. 3D Design of Fixed-Wing Hybrid Tricopter UAV

The Hybrid Tricopter VTOL UAV design offers several significant advantages that make it an ideal solution for precision agriculture applications. Its hybrid configuration enables operations in diverse environments, providing exceptional flexibility for tasks such as data collection, monitoring, and surveying. The Fixed-Wing Mode significantly enhances energy efficiency, enabling longer mission durations, while the VTOL capability simplifies deployment in remote or rugged terrains. Precision navigation is achieved through advanced sensors and control systems, ensuring high accuracy and reliability in various operational scenarios. Moreover, the use of 3D-printed materials and modular components minimizes production costs, offering a cost-effective solution without compromising performance. These features collectively position the UAV as a transformative tool for improving productivity and sustainability in agriculture. A detailed view of the UAV's 3D design and rendered model, which showcases the system's structural and mechanical layout, can be observed in Figure 5, providing a comprehensive visual representation of the proposed design.

D. Proposed Method

The Hybrid VTOL UAV, designed with a tricopter configuration, can be approximated as a rigid body due to its relative size and structural integrity compared to its surrounding environment. This model incorporates the six degrees of freedom (6-DoF) nonlinear equations of motion to comprehensively describe its dynamics. These equations are derived from Newton's Second Law of Motion, which governs translational dynamics, and Euler's equations, which are applied to capture the rotational dynamics.

$$\sum \vec{F} = m\frac{d\vec{V}}{dt} \tag{1}$$

$$\sum \vec{M} = I\frac{dH}{dt} \tag{2}$$

Extending from the foundational dynamics of the Hybrid VTOL UAV in its tricopter configuration, the forces and moments acting on the UAV are categorized into three primary components: aerodynamic, propulsive, and external forces and moments. Aerodynamic forces arise from the interaction between the UAV's structure and the surrounding air, affecting lift, drag, and stability. Propulsive forces and moments are generated by the rotors and propellers, which are crucial for providing thrust and controlling movement. Additionally, external forces and moments, such as gravitational effects and environmental disturbances like wind, play a critical role in influencing the UAV's stability and overall flight performance. These components have been formulated into mathematical equations as follows:

$$X = X_a + X_t + X_{\text{other}} \tag{3}$$

$$Y = Y_a + Y_t + Y_{\text{other}} \tag{4}$$

$$Z = Z_a + Z_t + Z_{\text{other}} \tag{5}$$

$$L = L_a + L_t + L_{\text{other}} \tag{6}$$

$$M = M_a + M_t + M_{\text{other}} \tag{7}$$

$$N = N_a + N_t + N_{\text{other}} \tag{8}$$

In hover mode, the impact of aerodynamic forces and moments is relatively minimal, making their contribution negligible in the mathematical modeling of the system. As a result, these factors are excluded from the analysis to simplify the equations without compromising accuracy. Conversely, the propulsive forces and moments play a dominant role in maintaining stability and controlling the UAV in this mode. These forces and moments are directly influenced by the thrust generated by each motor, the angular orientation of the motors, and the torque produced during operation. This dependency highlights the critical interplay between the propulsion system's parameters and the UAV's overall dynamic behavior, particularly during hover conditions.

Propulsive Forces:

$$X_t = T_1 \sin(-\sigma_1) + T_2 \sin(-\sigma_2) \tag{9}$$

$$Y_t = T_3 \sin(\zeta) \tag{10}$$

$$Z_t = -T_1 \cos(\sigma_1) - T_2 \cos(\sigma_2) - T_3 \cos(\zeta) \tag{11}$$

Propulsive Moments:

$$L_t = T_1 \cos(\sigma_1)\, r_y - T_2 \cos(\sigma_2)\, r_y + T_3 \sin(\zeta)\, r_z^{aft} + Q_2 \sin(-\sigma_2) - Q_1 \sin(-\sigma_1) \tag{12}$$

$$M_t = T_1 \cos(\sigma_1)\, r_x + T_2 \cos(\sigma_2)\, r_x - T_3 \cos(\zeta)\, r_x^{aft} - T_1 \sin(-\sigma_1)\, r_z - T_2 \sin(-\sigma_2)\, r_z - Q_3 \sin(\zeta) \tag{13}$$

$$N_t = T_1 \sin(-\sigma_1)\, r_x - T_2 \sin(-\sigma_2)\, r_x - T_3 \sin(\zeta)\, r_x^{aft} + Q_2 \cos(\sigma_2) - Q_1 \cos(\sigma_1) + Q_3 \cos(\zeta) \tag{14}$$

In this model, the propulsion system is represented by three primary rotors, denoted as Rotor 1, Rotor 2, and Rotor 3, corresponding to the left, right, and rear rotors, respectively. The thrust (T) and torque (Q) produced by these rotors serve as critical inputs to the system, directly influencing the UAV's dynamics. The angular orientations of the motors are represented by σ_1, σ_2 and ζ, which correspond to the angles of the front left motor, front right motor, and rear motor, respectively. These parameters play a pivotal role in determining the propulsive forces and moments that govern the UAV's stability and motion. The derived force and moment equations, accounting for these parameters, are subsequently incorporated into the comprehensive non-linear six degrees of freedom (6-DoF) model. This model provides a detailed mathematical framework for analyzing the UAV's behavior

under various operating conditions, ensuring an accurate representation of its translational and rotational dynamics.

Force Equations:

$$\dot{u} = \frac{X}{m} - g\sin(\theta) + rv - qw \tag{15}$$

$$\dot{v} = \frac{Y}{m} + g\cos(\theta)\sin(\phi) - ru + pw \tag{16}$$

$$\dot{w} = \frac{Z}{m} + g\cos(\theta)\cos(\phi) + qu - pv \tag{17}$$

Kinematic Equations:

$$\dot{\phi} = p + q\tan(\theta)\sin(\phi) + r\tan(\theta)\cos(\phi) \tag{18}$$

$$\dot{\theta} = q\cos(\phi) - r\sin(\phi) \tag{19}$$

$$\dot{\psi} = q\sec(\theta)\sin(\phi) + r\sec(\theta)\cos(\phi) \tag{20}$$

Moment Equations:

$$\dot{p} = \frac{I_{zz}L + I_{xz}N - \left(I_{xz}\left(I_{yy} - I_{xx} - I_{zz}\right)\right)p + \left(I_{xz}^2 + I_{zz}\left(I_{zz} - I_{yy}\right)\right)r}{I_{xx}I_{zz} - I_{xz}^2}q \tag{21}$$

$$\dot{q} = \frac{M - (I_{xx} - I_{zz})pr - I_{xx}(p^2 - r^2)}{I_{yy}} \tag{22}$$

$$\dot{r} = \frac{I_{xx}L + I_{xz}N - \left[I_{xz}\left(I_{yy} - I_{xx} - I_{zz}\right)r + \left(I_{xz}^2 + I_{xx}\left(I_{xx} - I_{yy}\right)\right)p\right]}{I_{xx}I_{zz} - I_{xz}^2} \tag{23}$$

Specifically, u, v, and w denote the linear velocity components along the x, y, and z axes, respectively, while p, q, and r represent the angular velocity components about the same axes. The orientation of the UAV is captured through the Euler angles ϕ, θ, and ψ which describe roll, pitch, and yaw, respectively. The external forces acting on the system are represented by X, Y, and Z corresponding to the net forces along the three axes. Additionally, the system's rotational dynamics are governed by moments L, M, and N which represent the torques about the respective axes and serve as critical inputs to the model. This comprehensive state representation ensures that all relevant aspects of the UAV's motion are accurately captured and analyzed within the framework of the six degrees of freedom (6-DoF) equations.

The dynamic behavior and stability of the Hybrid Tricopter VTOL UAV are heavily influenced by the effectiveness of its control system. Given the complexity of operating in multiple flight modes—hover, transition, and cruise—precise control mechanisms are required to manage the UAV's orientation and position. The non-linear characteristics of the UAV's dynamics, combined with external disturbances

such as wind or sudden shifts in thrust distribution, necessitate the use of robust control techniques to ensure stability and responsiveness.

To achieve this, Proportional-Integral-Derivative (PID) control systems are employed, forming the backbone of the UAV's flight control architecture. PID controllers are well-suited for UAV applications due to their ability to provide real-time corrections based on feedback signals, minimizing error and enhancing stability. The implementation of PID controllers in the tricopter configuration is critical for regulating its roll, pitch, and yaw dynamics. These controllers ensure the UAV maintains its intended flight trajectory and responds effectively to external inputs or disturbances.

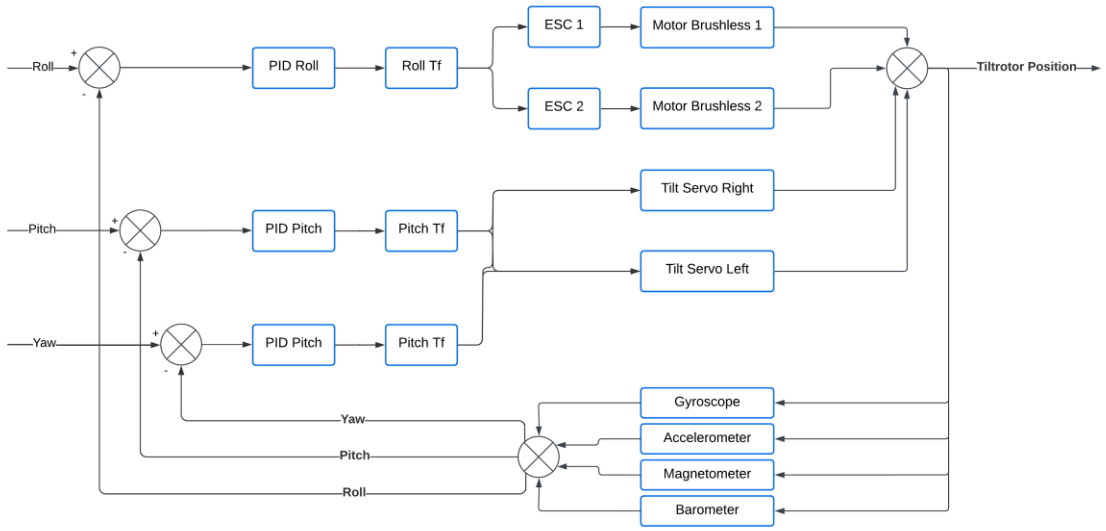

Figure 6. PID Control System of Fixed-Wing Hybrid Tricopter UAV

The Figure 6 illustrates the integration of PID controllers into the control architecture of the tricopter UAV, focusing on its roll, pitch, and yaw dynamics. At the core of the system are three PID controllers, each dedicated to one of the primary rotational axes: roll, pitch, and yaw. These controllers receive error signals generated by the difference between the desired and actual states of the UAV, which are derived from onboard sensors. The controllers process these signals to generate corrective commands, ensuring the UAV maintains its stability and adheres to the commanded orientation.

For roll control, the PID controller processes the roll error signal and outputs commands to the electronic speed controllers (ESCs) connected to the left and right motors. These motors, driven by the ESCs, adjust their thrust levels to achieve the desired roll position. Similarly, the pitch PID controller regulates the pitch dynamics by managing the tilt servos that control the angular position of the motors. The output from this controller ensures that the UAV can perform forward and backward tilting motions, enabling precise pitch adjustments.

The yaw dynamics are controlled by another PID controller, which interacts with the rear motor and the tilt mechanism. This controller ensures that the UAV maintains the desired heading by adjusting the torque and thrust distribution across

the rotors. The combination of yaw, roll, and pitch control provides the tricopter with the ability to maneuver in three-dimensional space with high precision.

Feedback from various onboard sensors plays a vital role in this control architecture. The gyroscope, accelerometer, magnetometer, and barometer provide real-time data on the UAV's orientation, acceleration, magnetic heading, and altitude, respectively. This sensor data is aggregated and processed to determine the current state of the UAV, forming the input for the PID controllers. By continuously comparing the desired states with the actual measurements, the controllers can dynamically adjust the motor outputs and servo positions, ensuring stable and accurate flight performance.

The PID control architecture shown in the Figure 6 represents a sophisticated system designed to manage the tricopter's complex dynamics. By leveraging feedback from multiple sensors and applying corrective actions through the ESCs and tilt servos, the system achieves precise and stable control of the UAV's roll, pitch, and yaw axes. This level of control is essential for the tricopter's performance, particularly in maintaining stability during hover, executing smooth transitions, and achieving reliable forward flight in fixed-wing mode.

E. Result and Discussion

This section presents the outcomes of the research and evaluates the performance of the UAV's control system and electronic components based on the conducted experiments. The analysis focuses on the results of two key missions: the hover mission and the transition mission, which were designed to assess the UAV's stability, responsiveness, and control accuracy across different flight modes. The performance of the implemented PID controllers is examined in maintaining precise roll, pitch, and yaw dynamics during the hover mission, while the transition mission evaluates the system's ability to seamlessly shift between hover and fixed-wing flight modes under varying tilt rates. Furthermore, the suitability of the selected electronic components, including motors, ESCs, sensors, and servos, is assessed based on their contribution to the UAV's overall performance. These experiments provide valuable insights into the robustness of the control design and the reliability of the UAV's architecture in meeting the operational demands of a hybrid VTOL system.

The results obtained from simulations and experimental tests are critically analyzed to highlight the system's strengths and identify areas for improvement. Particular attention is given to the precision of the PID controllers in minimizing errors and achieving stability, as well as the robustness of the electronic components in handling the demanding requirements of a hybrid UAV platform. To ensure a controlled and reliable environment for performance evaluation, the PID testing in this research was conducted using MATLAB simulations. These simulations provided a comprehensive platform for modeling the UAV's dynamics and testing the PID controllers' effectiveness in various scenarios before potential physical implementation. This discussion aims to provide a comprehensive understanding of the UAV's overall performance and its potential for real-world applications.

1. Electronic Component Performance Simulation

The eCalc Propeller Calculator (propCalc) serves as a critical tool for simulating and analyzing the performance of propellers within UAV systems. This software module enables precise calculations of essential parameters, such as thrust, power consumption, efficiency, and rotational speed, based on the selected motor, propeller, and environmental conditions. By incorporating aerodynamic properties and motor-propeller interactions, propCalc allows for detailed optimization of propulsion systems, ensuring compatibility and efficiency in real-world applications. In the context of this research, propCalc was used to evaluate the suitability of the propellers and motors for the Hybrid Tricopter VTOL UAV, providing valuable insights into the propulsion system's overall performance and its ability to meet the requirements for stable flight and efficient energy consumption. This tool plays a pivotal role in minimizing design uncertainties and ensuring the reliability of the UAV's propulsion system.

The parameter configuration used in the eCalc Propeller Calculator (propCalc) is tailored to simulate the propulsion system for the Hybrid Tricopter VTOL UAV. The model weight is set to 3300 grams, inclusive of the drive system, with three motors configured on a shared battery system. The battery specifications include a 10,000mAh LiPo cell with a 25C/35C discharge rating, providing sufficient capacity and current output for stable operations. The controller is configured for a maximum current of 50A, with a resistance of 0.005 ohms, ensuring efficient power delivery. The motor selected is a SunnySky X2216-950 V3, providing a no-load current of 0.7A and a resistance of 0.0736 ohms, paired with a GemFan propeller featuring a 9-inch diameter and a 6-inch pitch. Additional settings include a wingspan of 1450mm, a drag coefficient of 0.033, and environmental parameters such as a field elevation of 250m and standard air pressure (QNH 1013 hPa). Another critical parameter is the flight speed, initially set to 0 km/h in the simulation. However, subsequent evaluations will involve adjusting the flight speed to 60 km/h to analyze the propulsion system's behavior under dynamic flight conditions. These comprehensive settings provide a detailed and precise simulation environment to analyze the UAV's propulsion performance. The complete configuration details can be observed in Figure 7, which visually represents the key parameters set for the simulation.

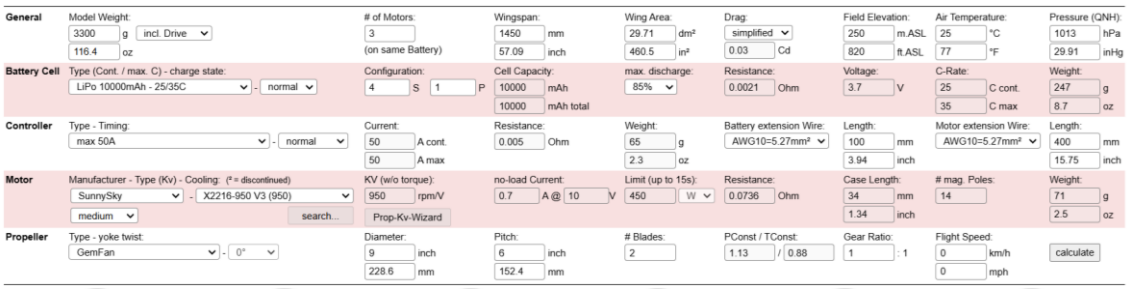

Figure 7. Simulation Setting of Cruise Motor

The simulation results from the configured parameters provide comprehensive insights into the performance of the propulsion system for the Hybrid Tricopter VTOL UAV. The load is calculated at 6.6C, indicating the discharge rate of the battery relative to its capacity, while the mixed flight time is estimated to

be 14.0 minutes, balancing between hover and forward flight modes. The electric power consumption is measured at 311 watts, highlighting the power demands of the propulsion system under the given conditions. The estimated temperature reaches 53°C, showcasing the thermal characteristics of the motors and ESCs under continuous operation. The thrust-to-weight ratio is calculated at 1.22, indicating the UAV's ability to achieve vertical lift and maintain stable flight. The pitch speed, which affects forward velocity and maneuverability, is estimated to reach a peak of 102 km/h, demonstrating the propulsion system's capacity for efficient flight dynamics in forward motion. The complete details can be observed in Figure 8.

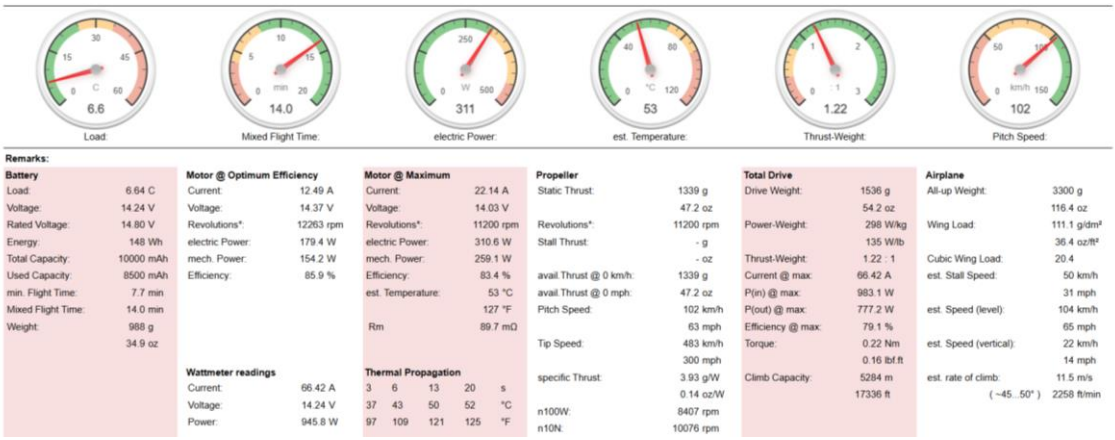

Figure 8. Simulation Results of Cruise Motor

Additional metrics provide further evaluation of system performance. The battery status highlights a usable capacity of 8500mAh, with a total energy output of 148 Wh during operation. At optimal efficiency, the motors draw a current of 12.42A, generating 154.2 watts of mechanical power at 12,623 RPM, with an efficiency rate of 85.9%. At maximum output, the motors operate at 14.03V, producing 285.1W of mechanical power at 11,200 RPM, with an estimated temperature rise to 127°F under high load. The propeller provides a static thrust of 1339g at 11,200 RPM, with a specific thrust of 3.93 g/W, emphasizing the system's efficiency in converting power to thrust. The overall climb capacity of the UAV is calculated at 5284 m, while the estimated rate of climb reaches 11.5 m/s, showcasing the UAV's ability to ascend rapidly and efficiently. These simulation results, which cover critical performance metrics, validate the suitability of the configured parameters for the Hybrid Tricopter VTOL UAV and provide a robust basis for further optimization and testing.

The Motor Characteristics at Full Load graph provides a detailed representation of the motor's performance under maximum operating conditions. Each line on the graph corresponds to a critical performance parameter, allowing for an in-depth evaluation of the motor's behavior:

a) Electrical Power (in 2W): Represented by the yellow line, this curve shows the electrical power input to the motor as the current increases. The line demonstrates a steady increase with the current, reaching its peak at approximately 175 W. This indicates the motor's capacity to handle high power input efficiently under full load without surpassing its limits.

b) Efficiency (%): The blue line represents the motor's efficiency, peaking at moderate current levels and then gradually decreasing as the current increases. This trend is expected as efficiency tends to drop at higher loads due to increased thermal and mechanical losses. The motor maintains a high efficiency across most of its operational range, reflecting its capability to convert electrical power into mechanical power effectively.
c) Maximum Revolutions (in 100rpm): Depicted by the purple line, this curve shows the maximum rotational speed of the motor. The line maintains a nearly constant trend, demonstrating that the motor can sustain consistent RPM even as the current increases. This stability is crucial for ensuring predictable performance in UAV applications.
d) Waste Power (in W): The orange line shows the power lost due to inefficiencies, such as heat dissipation and friction. As expected, this line increases with current, highlighting the need for effective thermal management to maintain motor performance over extended operations.
e) Motor Case Temperature (°C): Represented by the green line, this curve indicates the motor's case temperature as the current increases. The motor's temperature remains well within safe limits throughout the operating range, reflecting adequate thermal stability under full load.
f) Motor Case Temperature Overlimit (°C): The red dashed line, representing the thermal safety limit, is never approached by the motor case temperature line (green), confirming that the motor operates within its thermal safety margins during full load conditions.

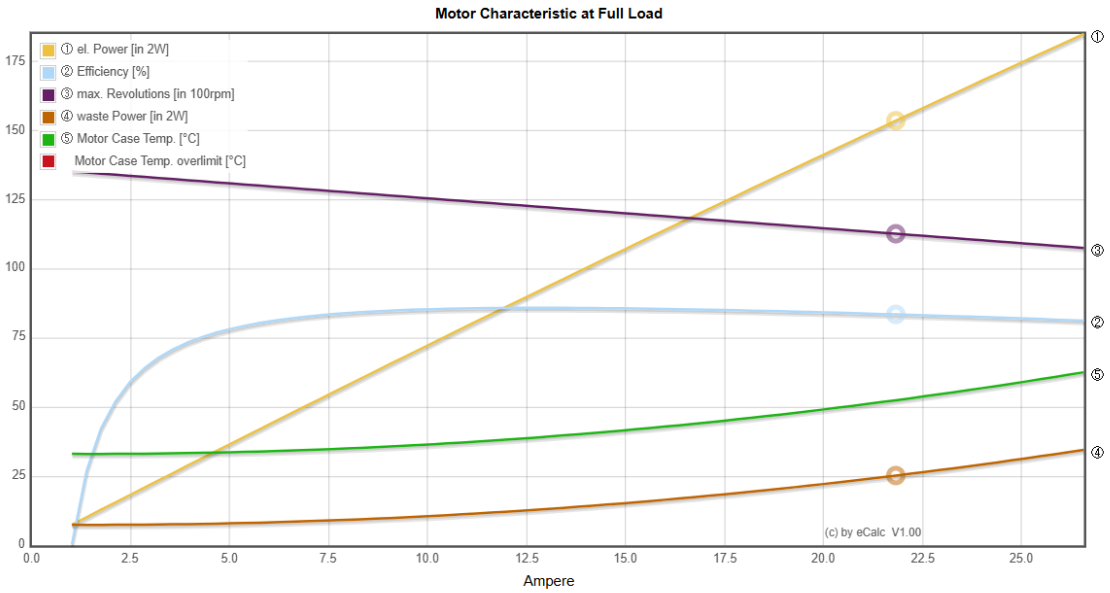

Figure 9. Graph of Simulation Results - Motor Characteristics at Full Load

The detailed representation of the motor's characteristics under full load conditions can be observed in Figure 9, which visually illustrates the motor's behavior and confirms its operational safety and efficiency within the defined parameters. This graph complements the simulation results by confirming the motor's capability to operate under full load without exceeding thermal or efficiency

thresholds. The consistency and stability across the parameters validate the suitability of the selected motor for the Hybrid Tricopter VTOL UAV, ensuring reliable performance and durability in demanding applications.

Building on the analysis of the motor's performance under full load conditions, it is equally important to evaluate its thermal behavior over time to ensure sustained operational reliability. The Thermal Propagation at Full Load graph in Figure 10 provides a comprehensive view of how the motor manages heat generation during extended operation. This analysis serves as a critical complement to the previously discussed motor characteristics, as thermal stability directly impacts the motor's long-term durability and performance in real-world applications.

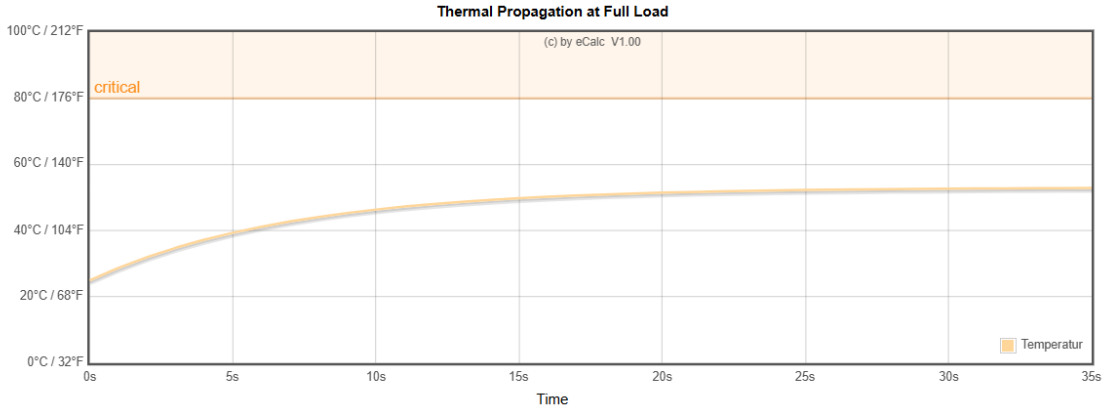

Figure 10. Graph of Simulation Results – Thermal Propagation at Full Load

The Thermal Propagation at Full Load graph illustrates the temperature progression of the motor over time when operating at maximum load. The temperature curve rises steadily during the initial seconds of operation, indicating the heat generated by electrical and mechanical losses within the motor. However, the graph demonstrates that the temperature levels off well below the critical threshold of 80°C, even after extended operation of 35 seconds. This behavior highlights the motor's thermal stability and efficient heat dissipation capabilities under full load conditions. The gradual increase without exceeding the critical temperature range ensures the motor operates safely without risking thermal damage. These results confirm the effectiveness of the motor's thermal design and its suitability for the demanding operational requirements of the Hybrid Tricopter VTOL UAV. The findings underscore the motor's reliability for sustained performance, validating its integration into the propulsion system for high-intensity applications.

The simulation results of the electronic components, including the propulsion system and thermal behavior, demonstrate that the selected components are highly suitable for the Hybrid Tricopter VTOL UAV. The motor and propeller configurations, validated through tools like eCalc, exhibit excellent efficiency, stable performance, and the ability to operate within safe thermal limits under full load conditions. The thermal propagation analysis further confirms the motor’s capacity to manage heat effectively without exceeding critical thresholds, ensuring reliable long-term operation. These findings suggest that the electronic components, as configured in the simulations, possess the quality and reliability required for real-

world implementation, providing confidence in their ability to meet the rigorous demands of precision UAV applications in diverse environmental and operational scenarios.

2. Simulation of UAV Control Design

The system depicted in Figure 11 represents the overall control architecture for the Hybrid Tricopter VTOL UAV, showcasing the integration of multiple control components to facilitate smooth transitions between hover and fixed-wing flight modes. At its core, the control system employs a Multiplexer Controller to manage commands from different flight modes, including hover commands and manual controls. Sensor data, processed through a filter or estimator, is used to generate estimated states, which are critical for decision-making across the system. The Tilt Scheduler module plays a pivotal role in transitioning between multicopter and fixed-wing modes, dynamically adjusting tilt angles and flight states based on the UAV's current operational status. Commands from the Tilt Scheduler are distributed to motor actuators and control surfaces via the Scheduler Module, which ensures synchronized operation between tilt rotors and fixed-wing components. This control architecture ensures seamless mode transitions, stability during operation, and precise maneuvering, even under complex environmental conditions.

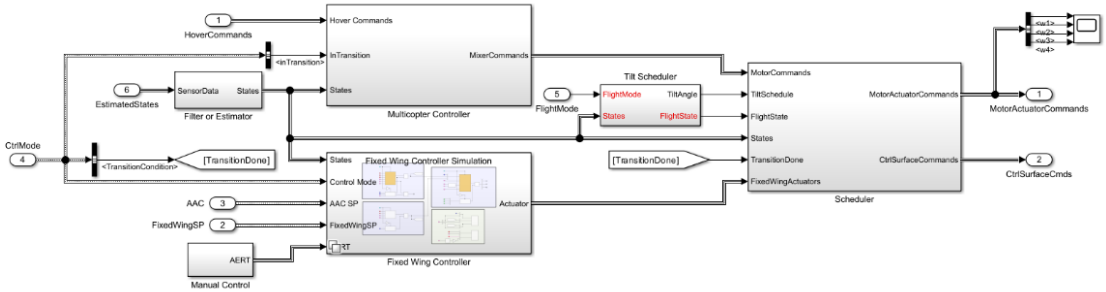

Figure 11. Control Architecture of UAV

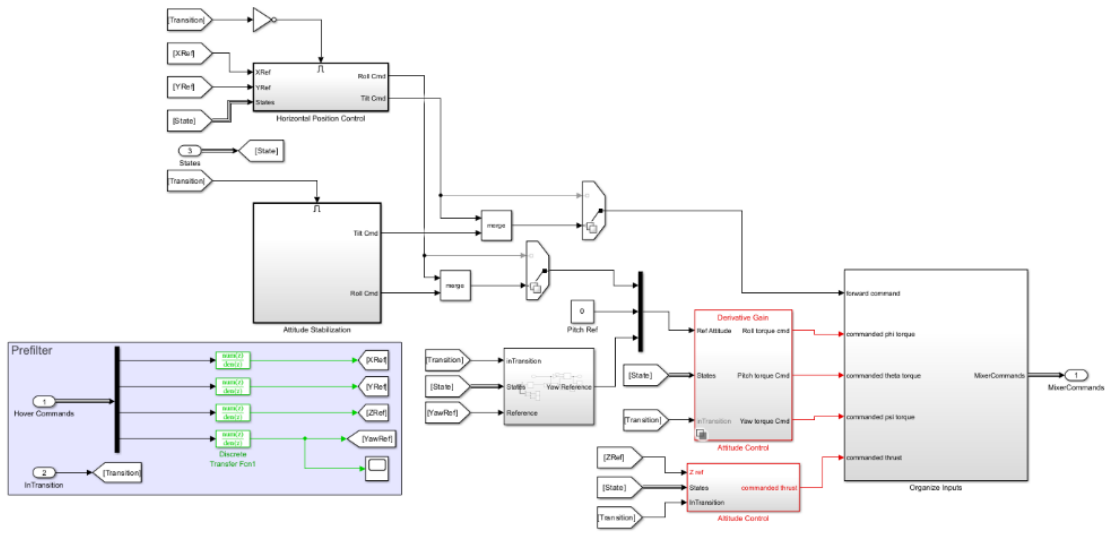

Figure 12. Multicopter Controller Module

Figure 12 elaborates on the Multicopter Controller module, which is responsible for stabilizing the UAV during hover and transition phases. The Prefilter component processes hover and transition commands, refining them into inputs suitable for attitude stabilization. The Attitude Stabilization block generates control signals for roll, pitch, and yaw axes based on reference values and feedback from sensors, ensuring precise control of the UAV's orientation. These commands are further refined through various processing blocks to calculate the appropriate torque and thrust values for each rotor. The multicopter controller is particularly critical during hover and vertical takeoff or landing, where maintaining stability and responding to environmental disturbances require precise and rapid adjustments.

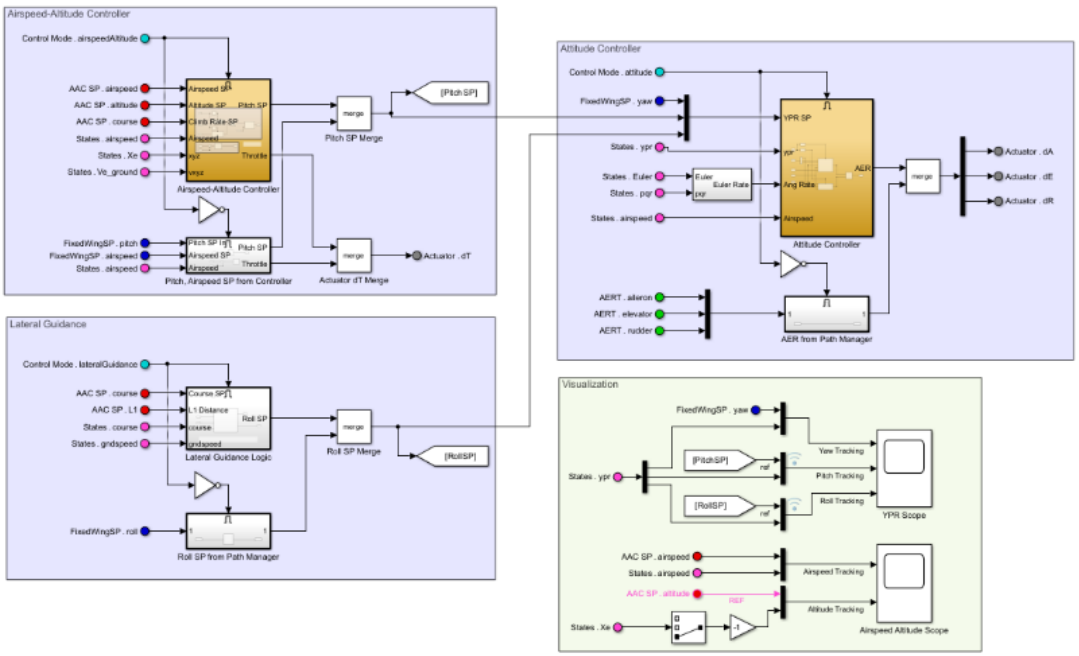

Figure 13. Fixed-Wing Controller Module

Figure 13 focuses on the Fixed-Wing Controller, which governs the UAV's performance during forward flight. The system is divided into three key sections: Airspeed-Attitude Controller, Lateral Guidance, and Altitude Controller. The Airspeed-Attitude Controller ensures the UAV maintains its desired speed and pitch attitude, merging throttle and pitch inputs for smooth adjustments. The Lateral Guidance module provides roll control for directional changes, enabling the UAV to follow predefined paths accurately. Meanwhile, the Altitude Controller manages vertical positioning, combining Euler angle data with altitude references to maintain consistent flight levels. Visualization tools are integrated into this system, allowing real-time tracking of yaw, pitch, roll, and airspeed parameters for monitoring and debugging purposes. This modular structure ensures that the UAV achieves optimal performance, stability, and responsiveness during fixed-wing operations.

The provided diagram represents the implementation of PID controllers for roll and pitch control within the UAV's flight control system. This architecture demonstrates a hierarchical control approach, where angular position and rate are

managed separately to achieve precise and stable attitude control. The specific configuration and operation of the PID controllers, including their cascaded structure and parameter tuning, can be observed in Figure 14, which provides a detailed visualization of how the controllers interact to achieve robust and responsive attitude stabilization.

The Roll Control module consists of two cascaded controllers: the Roll Angle Controller and the Roll Rate Controller. The roll setpoint ($RollSP$) is compared with the current roll angle to generate an error signal. This error is processed by the Roll Angle Controller, which is a proportional controller $P(z/r)$, generating a target roll rate. The target roll rate is then compared to the actual roll rate, and the resulting error is passed to the Roll Rate Controller, also a proportional controller $P(z/r)$. This cascade structure ensures precise roll adjustments by dynamically correcting both angular position and rate.

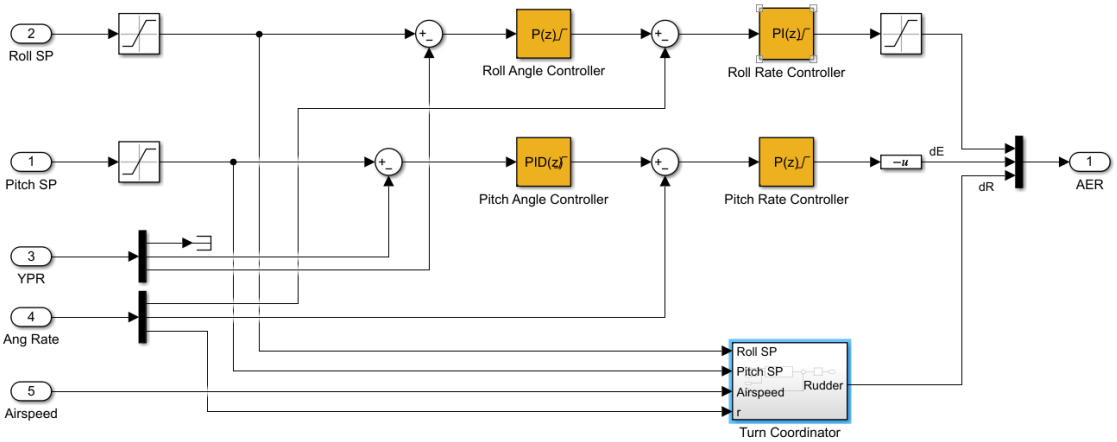

Figure 14. PID Controller on Pitch and Roll

Similarly, the Pitch Control module operates with a Pitch Angle Controller and a Pitch Rate Controller. The pitch setpoint ($PitchSP$) is compared with the current pitch angle, and the resulting error is processed through the Pitch Angle Controller, a PID controller $PID(z/r)$. This controller generates a target pitch rate, which is then compared with the actual pitch rate, and the error is processed through the Pitch Rate Controller $P(z/r)$. This structure enables smooth and stable control of the UAV's pitch dynamics.

Additional inputs, such as Yaw-Pitch-Roll (YPR) angles, angular rates ($AngRate$), and airspeed ($Airspeed$), feed into the Turn Coordinator module. This module integrates these parameters to adjust control outputs dynamically, ensuring coordinated turns and overall stability during flight. The output signals from the controllers (dE, dR) are combined and sent to the UAV's actuators (AER) to apply the necessary control inputs to maintain or adjust the UAV's attitude as per the setpoints. This cascaded PID control structure provides a robust mechanism for achieving precise and responsive attitude control, ensuring stability and smooth performance across various flight modes and conditions.

The hover mission serves as a critical test to evaluate the performance and stability of the UAV's control system in maintaining precise positional control across three dimensions: X (horizontal), Y (lateral), and Z (vertical). This experiment is

designed to validate the responsiveness of the implemented control algorithms, particularly the PID controllers, in tracking commanded trajectories and minimizing positional errors. By analyzing the UAV's ability to follow command inputs while counteracting disturbances, the hover mission provides essential insights into the effectiveness of the control architecture and its readiness for real-world applications. The results of this test, as illustrated in the following figures, highlight the system's accuracy and robustness in achieving stable hover performance.

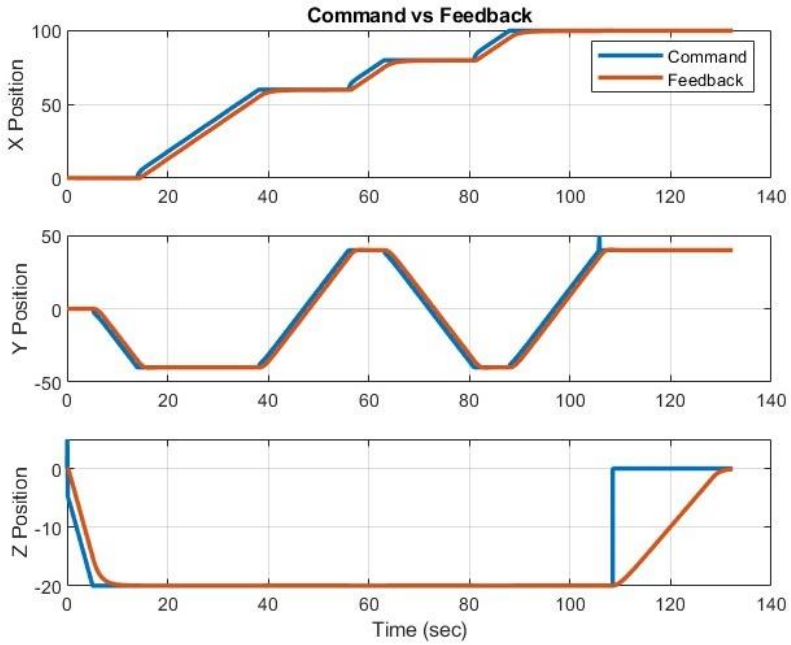

Figure 15. Command vs Feedback Across the X, Y, and Z positions

Figure 15 illustrates the comparison between the command inputs and the system's feedback responses across the X, Y, and Z positions during the hover mission. The blue lines represent the commanded trajectories, while the orange lines indicate the feedback, which reflects the actual response of the UAV. The results demonstrate a high level of correspondence between the command and feedback, with only minimal deviations observed, particularly during dynamic transitions. In the X and Y axes, the UAV closely tracks the commanded positions, maintaining precise horizontal control. The Z axis, representing altitude, shows a slight lag during initial ascent and transition phases, but stabilizes as the UAV approaches the commanded position. These results validate the effectiveness of the control system in executing hover missions with high positional accuracy.

Figure 16 presents the error between the command inputs and the feedback responses for the X, Y, and Z positions over time. The error remains minimal throughout the mission, with transient spikes occurring during transitions and sharp directional changes. In the X and Y axes, the error is less than 5 units, indicating precise horizontal control. The Z axis error, primarily during the initial ascent, reaches a peak of approximately 10 units before converging to near-zero as the altitude stabilizes. This analysis confirms that the control system effectively minimizes positional discrepancies, ensuring reliable and stable performance during the hover mission.

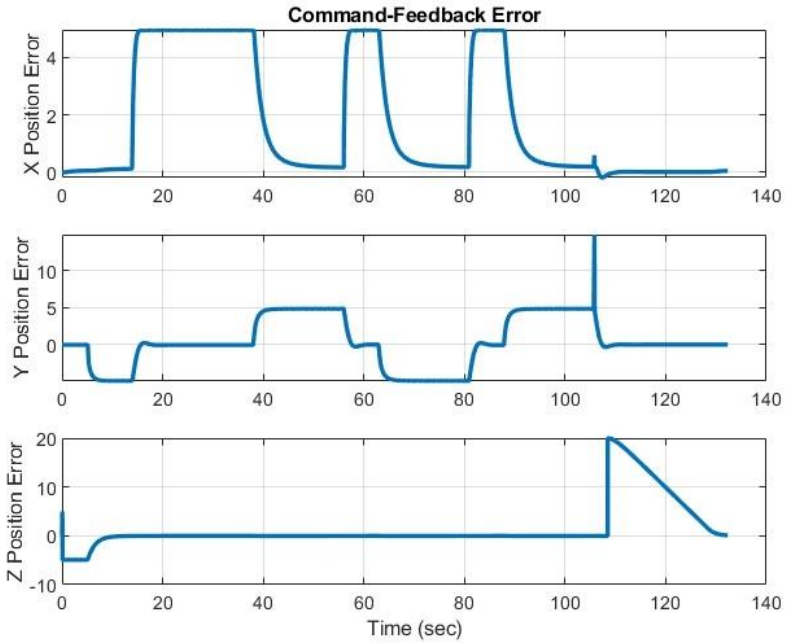

Figure 16. Command Feedback Error on UAV Simulation

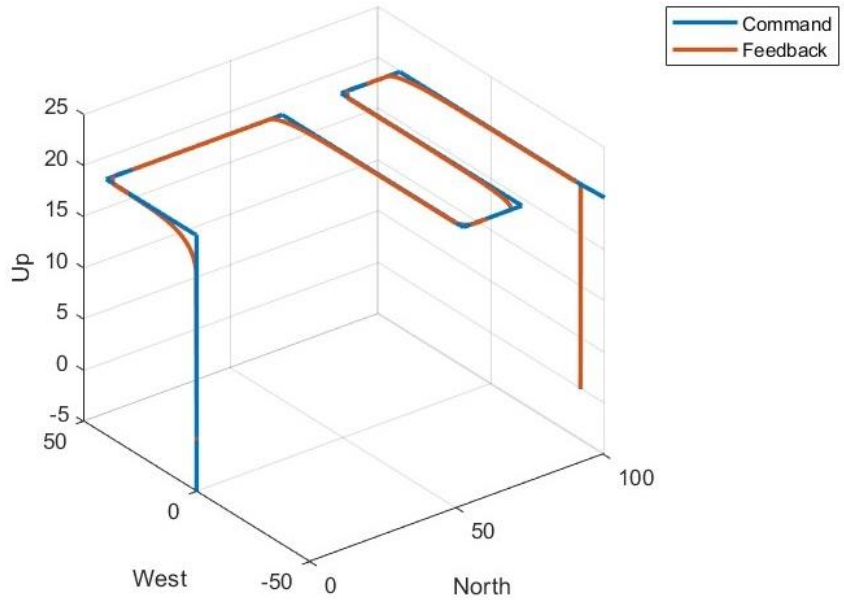

Figure 17. 3D Trajectory of UAV in Hover Mission

Figure 17 provides a 3D visualization of the UAV's trajectory during the hover mission, highlighting the command (blue line) and feedback (orange line) paths. The UAV demonstrates excellent adherence to the commanded trajectory, accurately transitioning between waypoints in the X, Y, and Z dimensions. Minor deviations are observed during altitude changes, particularly during the initial ascent, but these discrepancies are quickly corrected. The overall trajectory indicates a well-coordinated response from the control system, with the UAV successfully executing the mission objectives while maintaining stability and precision. This 3D

perspective offers a comprehensive view of the UAV's positional control, further validating the robustness of the implemented control design.

The transition mission is a critical evaluation designed to test the UAV's ability to smoothly transition between hover and fixed-wing flight modes, a key feature of hybrid VTOL systems. This experiment assesses the control system's performance in managing the dynamic changes in aerodynamic forces, thrust distribution, and attitude adjustments that occur during the transition phase. By analyzing the UAV's response to varying tilt rates and its ability to maintain stability and achieve target flight conditions, the transition mission provides valuable insights into the robustness and adaptability of the implemented control design. The results of this test, as illustrated in the following figures, highlight the effectiveness of the UAV's control system in executing complex transitions while maintaining operational reliability and precision.

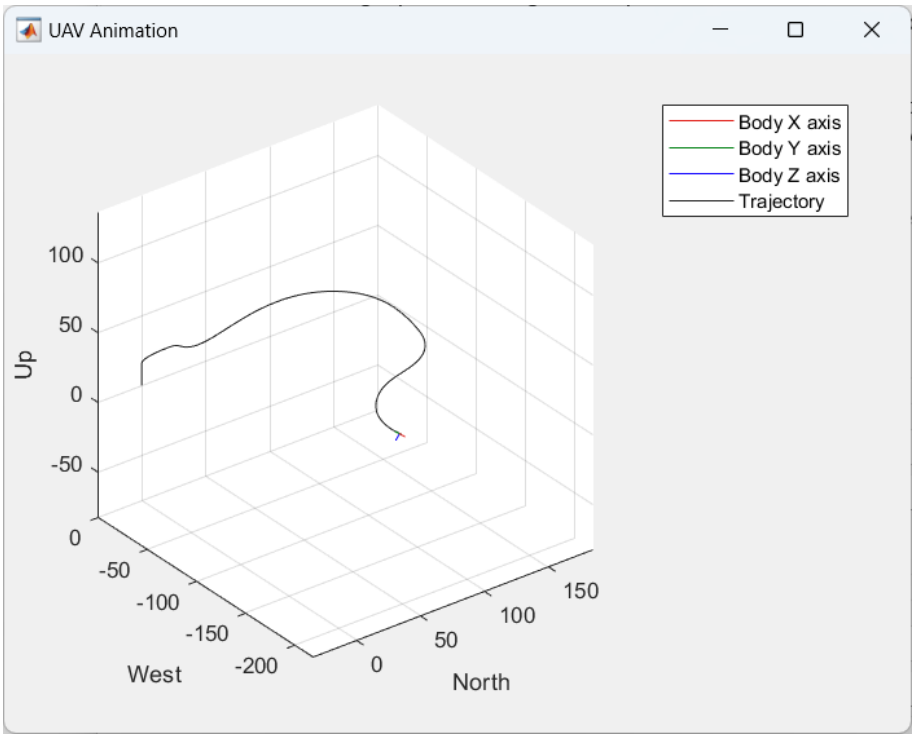

Figure 18. 3D Trajectory of UAV in Transition Mission

Figure 18 visualizes the UAV's 3D trajectory during the transition mission, highlighting its ability to transition smoothly between hover and fixed-wing modes. The trajectory line represents the UAV's path in the North, West, and vertical (Up) directions, while the colored axes indicate the body-fixed frame's orientation. The trajectory shows a gradual and controlled adjustment as the UAV transitions from a stable hover into forward flight. The trajectory curvature and consistent altitude adjustments indicate a precise response from the control system, ensuring stability and smooth movement during the transition. This behavior validates the capability of the UAV to maintain balanced and reliable control while shifting between distinct flight modes, a critical requirement for hybrid VTOL operations.

Figure 2 presents the dynamics of the UAV's transition under different tilt rates (15°/sec, 30°/sec, and 45°/sec). The four plots display the variations in altitude, pitch angle, tilt angle, and airspeed over time.

a) Altitude (Top Plot): Across all tilt rates, the UAV steadily gains altitude during the transition, with minor variations observed. The consistency in altitude change demonstrates the robustness of the control system in maintaining vertical stability during the mode shift.
b) Pitch Angle (Second Plot): The pitch dynamics exhibit sharper variations at higher tilt rates, particularly at 30°/sec and 45°/sec. This indicates increased angular momentum at faster transitions, which requires the control system to implement more aggressive corrections to stabilize the UAV.
c) Tilt Angle (Third Plot): The tilt angle demonstrates a rapid adjustment to the desired configuration as the UAV transitions into forward flight. Higher tilt rates achieve the target tilt angle more quickly but also introduce transient disturbances, which are effectively mitigated by the control system. Lower tilt rates, such as 15°/sec, result in smoother transitions with reduced disturbances, providing a trade-off between speed and stability.
d) Airspeed (Bottom Plot): The airspeed increases as the UAV completes the transition into forward flight. Higher tilt rates, such as 30°/sec and 45°/sec, achieve faster acceleration, whereas the 15°/sec tilt rate results in a more gradual increase in speed. This reflects the UAV's ability to adapt to different transition strategies, balancing between rapid response and operational smoothness.

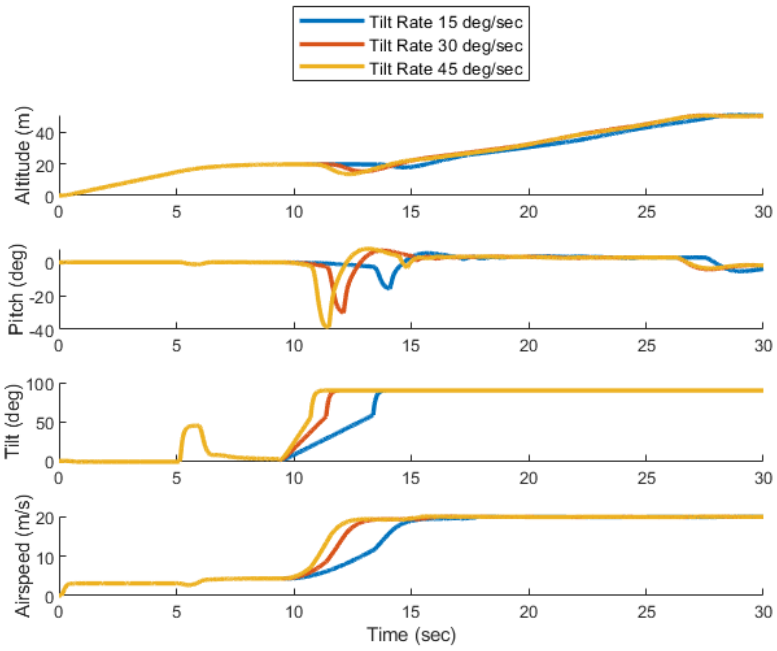

Figure 19. UAV Control System Performance in Varying Degrees of Tilt

Overall, Figure 19 demonstrates that the UAV's control system performs effectively under varying tilt rates, maintaining stability and achieving seamless transitions. Faster tilt rates provide quicker transitions but require more dynamic

corrections, whereas slower rates ensure smoother and more stable adjustments. These results validate the control system's flexibility and adaptability in managing transition dynamics, essential for hybrid VTOL operations.

F. Conclusion

This research has significantly contributed to advancing the development of UAV technology tailored for Precision Agriculture (PA), addressing the critical need for efficient and accurate farmland monitoring. The primary objective of this study—to design, simulate, and evaluate a Hybrid Tricopter VTOL UAV capable of performing data-driven agricultural tasks—was successfully achieved. By leveraging the UAV's ability to operate seamlessly in both hover and fixed-wing flight modes, was achieved through comprehensive simulation and testing.

The results of the hover and transition missions demonstrated the UAV's capability to maintain stability and precision during complex flight operations. The hover mission validated the effectiveness of the PID controllers in stabilizing the UAV's roll, pitch, and yaw dynamics, achieving high positional accuracy with minimal error rates. The transition mission further highlighted the UAV's adaptability, showcasing its ability to smoothly shift between hover and forward flight modes under varying tilt rates. These findings confirm the robustness and reliability of the implemented control system in meeting the demands of hybrid flight operations.

The integration and evaluation of key electronic components, including motors, ESCs, sensors, and servos, further reinforce the UAV's readiness for practical application. Simulation results revealed that the propulsion system operates efficiently within thermal and electrical thresholds, ensuring durability and sustained performance. The use of tools such as the eCalc Propeller Calculator enabled precise configuration and optimization of the UAV's propulsion parameters, demonstrating its suitability for long-duration and energy-efficient operations.

In the context of Precision Agriculture, this UAV system offers a practical solution for addressing critical challenges such as monitoring crop health, evaluating soil conditions, and optimizing resource allocation. By providing accurate, real-time data, the UAV empowers farmers and agricultural managers to make informed decisions, ultimately enhancing productivity and sustainability. This technology is particularly valuable in mitigating the effects of labor shortages, climatic variability, and declining agricultural areas, as evidenced by recent trends in rice production in Indonesia.

Overall, the outcomes of this research align closely with the goals of Precision Agriculture, contributing to the development of advanced, cost-effective UAV systems for farmland monitoring. While the system demonstrated high reliability and adaptability, it also opens avenues for future work, including the integration of specialized sensors for vegetation analysis, hydrological mapping, and pest monitoring. This study underscores the potential of UAVs to revolutionize agricultural practices, making them more efficient, data-driven, and sustainable in the face of evolving global challenges.

G. Acknowledgment

This research is supported and funded by the *"Direktorat Riset, Teknologi dan Pengabdian Kepada Masyarakat Kementerian Pendidikan, Kebudayaan, Riset, dan Teknologi"* based on Decree Number 459/E5/PG.02.00/2024 and Agreement/Contract Number 105/E5/PG.02.00.PL/2024; 823/LL3/AL.04/2024; 0/2/04.02/0793/07/2024.

H. References

[1] "Precision Ag Definition | International Society of Precision Agriculture," https://www.ispag.org/about/definition.

[2] A. O. Food, "of the United Nations, The future of food and agriculture, trends and challenges."

[3] P. Tamasiga, H. Onyeaka, M. Bakwena, A. Happonen, and M. Molala, "Forecasting disruptions in global food value chains to tackle food insecurity: The role of AI and big data analytics–A bibliometric and scientometric analysis," *J Agric Food Res*, vol. 14, p. 100819, 2023.

[4] M. A. M. Zawawi, S. Mustapha, and Z. Puasa, "Determination of water requirement in a paddy field at Seberang Perak rice cultivation area," *The Institution of Engineers, Malaysia [online]*, vol. 71, no. 4, pp. 33–41, 2010.

[5] "Luas Panen dan Produksi Padi di Indonesia 2023," https://www.bps.go.id/id/pressrelease/2024/03/01/2375/Luas-Panen-dan-Produksi-Padi-di-Indonesia-2023--Angka-Tetap-.html.

[6] S. K. Phang, T. H. A. Chiang, A. Happonen, and M. M. L. Chang, "From satellite to UAV-based remote sensing: A review on precision agriculture," *IEEE Access*, 2023.

[7] H. Shakhatreh *et al.*, "Unmanned aerial vehicles (UAVs): A survey on civil applications and key research challenges," *Ieee Access*, vol. 7, pp. 48572–48634, 2019.

[8] X. Li and L. Yang, "Design and implementation of UAV intelligent aerial photography system," in *2012 4th International Conference on Intelligent Human-Machine Systems and Cybernetics*, IEEE, 2012, pp. 200–203.

[9] P. J. Zarco-Tejada, M. L. Guillén-Climent, R. Hernández-Clemente, A. Catalina, M. R. González, and P. Martín, "Estimating leaf carotenoid content in vineyards using high resolution hyperspectral imagery acquired from an unmanned aerial vehicle (UAV)," *Agric For Meteorol*, vol. 171, pp. 281–294, 2013.

[10] Y. A. Pederi and H. S. Cheporniuk, "Unmanned aerial vehicles and new technological methods of monitoring and crop protection in precision agriculture," in *2015 IEEE International Conference Actual Problems of Unmanned Aerial Vehicles Developments (APUAVD)*, IEEE, 2015, pp. 298–301.

[11] A. Risnumawan *et al.*, "Automatic detection of wrecked airplanes from UAV images," *EMITTER International Journal of Engineering Technology*, vol. 7, no. 2, pp. 570–585, 2019.

[12] M. Bernard and K. Kondak, "Generic slung load transportation system using small size helicopters," in *2009 IEEE International Conference on Robotics and Automation*, IEEE, 2009, pp. 3258–3264.

[13] K. C. Swain, S. J. Thomson, and H. P. W. Jayasuriya, "Adoption of an unmanned helicopter for low-altitude remote sensing to estimate yield and total biomass of a rice crop," *Trans ASABE*, vol. 53, no. 1, pp. 21–27, 2010.
[14] P. E. I. Pounds, D. R. Bersak, and A. M. Dollar, "Stability of small-scale UAV helicopters and quadrotors with added payload mass under PID control," *Auton Robots*, vol. 33, pp. 129–142, 2012.
[15] Y. Lan, C. Shengde, and B. K. Fritz, "Current status and future trends of precision agricultural aviation technologies," *International Journal of Agricultural and Biological Engineering*, vol. 10, no. 3, pp. 1–17, 2017.
[16] D. Gómez-Candón, A. I. De Castro, and F. López-Granados, "Assessing the accuracy of mosaics from unmanned aerial vehicle (UAV) imagery for precision agriculture purposes in wheat," *Precis Agric*, vol. 15, pp. 44–56, 2014.
[17] J. Torres-Sánchez, F. López-Granados, A. I. De Castro, and J. M. Peña-Barragán, "Configuration and specifications of an unmanned aerial vehicle (UAV) for early site specific weed management," *PLoS One*, vol. 8, no. 3, p. e58210, 2013.
[18] J. Torres-Sánchez, F. López-Granados, N. Serrano, O. Arquero, and J. M. Peña, "High-throughput 3-D monitoring of agricultural-tree plantations with unmanned aerial vehicle (UAV) technology," *PLoS One*, vol. 10, no. 6, p. e0130479, 2015.
[19] R. Jannoura, K. Brinkmann, D. Uteau, C. Bruns, and R. G. Joergensen, "Monitoring of crop biomass using true colour aerial photographs taken from a remote controlled hexacopter," *Biosyst Eng*, vol. 129, pp. 341–351, 2015.
[20] T. Özaslan *et al.*, "Towards fully autonomous visual inspection of dark featureless dam penstocks using MAVs," in *2016 IEEE/RSJ International Conference on Intelligent Robots and Systems (IROS)*, IEEE, 2016, pp. 4998–5005.
[21] B. Dai, Y. He, F. Gu, L. Yang, J. Han, and W. Xu, "A vision-based autonomous aerial spray system for precision agriculture," in *2017 ieee international conference on robotics and biomimetics (ROBIO)*, IEEE, 2017, pp. 507–513.
[22] C. Peng, X. M. Wang, and X. Chen, "Design of tiltrotor flight control system in conversion mode using improved neutral network PID," *Adv Mat Res*, vol. 850, pp. 640–643, 2014.
[23] E. Irmawan, "Kendali Proses Transisi Hover To Cruise Pada Pesawat Tanpa Awak Vtol Fixed Wing," *Teknika STTKD: Jurnal Teknik, Elektronik, Engine*, vol. 4, no. 2, pp. 15–19, 2017.